On the kinetics of spontaneous amorphization of a metastable crystalline phase

2001 J. Phys.: Condens. Matter 13 7223

(http://iopscience.iop.org/0953-8984/13/33/304)

INSTITUTE OF PHYSICS PUBLISHING JOURNAL OF PHYSICS: CONDENSED MATTER

J. Phys.: Condens. Matter **13** (2001) 7223–7236 PII: S0953-8984(01)22085-2

On the kinetics of spontaneous amorphization of a metastable crystalline phase

N V Alekseechkin[1], **A S Bakai**[1] **and C Abromeit**[2]

[1] 'Kharkov Institute of Physics and Technology' National Science Centre, Akademicheskaya Street 1, Kharkov 61108, Ukraine
[2] Hahn-Meitner-Institut Berlin GmbH, Glienicker Strasse 100, D-14109 Berlin, Germany

E-mail: n.alex@kipt.kharkov.ua

Received 19 February 2001
Published 2 August 2001
Online at stacks.iop.org/JPhysCM/13/7223

Abstract

The phase transformations of a metastable crystalline phase obtained under high pressure occurring upon heating are considered: amorphization and subsequent crystallization. A model for the kinetics of these processes taking into account the capability for competitive formation of crystalline and amorphous phases at the boundaries of the grains of the initial phase is constructed. Expressions for the volume fractions as well as for the nucleation rates and growth velocities of the phases formed are obtained. Differential scanning calorimetry curves are described. A numerical analysis of the equations of the kinetics and a comparison with the results from experiment are carried out with reference to $Cd_{43}Sb_{57}$ alloy.

1. Introduction

Generally, a substance which is in a metastable state transforms over time and approaches a stable state (the state having the lowest free energy). If there are one or more metastable states with free energies lying between those of the initial state and final state, then the phase transformation occurs by a competitive formation of precipitates of the stable and intermediate metastable phases. The competitive formation of precipitates of several phases was considered in references [1–3]. Approximate solutions for the time dependence of the volume fractions of competing phases and of the size distribution functions of the precipitates were obtained. Also, the kinetics of transformation of supercooled liquids during cooling with competitive formation of crystalline and amorphous phases was considered and the dependence of the volume fractions of the amorphous and crystalline phases in the final state on the cooling rate was investigated.

Along with the formation of amorphous solids from supercooled liquids, the amorphization of metastable or non-equilibrium crystalline solid-state phases is also known to occur [4–7]. In [5, 7], amorphization of the high-pressure phases (HP phases) of some alloys, which are

semiconductors under ordinary conditions, was revealed and investigated experimentally. Here we consider the amorphization of Cd–Sb alloy. The experimental data concerning this alloy are given below.

In figure 1, the T–P diagram for the alloys mentioned above is shown. The HP phase, which is the metal γ-phase, exists at pressures $P \geqslant 5.0$ GPa. The γ-phase can be preserved for an indefinitely long time at liquid-nitrogen temperature and pressure $P = 1$ atm. Upon slow heating to room temperature, it transforms into an amorphous state. With further heating it crystallizes, reaching the equilibrium state. The solid lines in figure 1 represent the low-pressure (A_nB_m) and high-pressure (γ-phase) melting curves, dashed lines are extensions of the melting curves to the metastable region, the dash–dotted line corresponds to the equilibrium $A_nB_m \rightleftharpoons \gamma + B$, the shaded bands show the kinetic regions of the phase transformations $A_nB_m \rightarrow \gamma + B$ and $\gamma + B \rightarrow A_nB_m$. The authors of [5, 7] explain the amorphization phenomenon as follows. When the b_1b_2 section of the virtual melting curve passes below the phase transition kinetic band, upon intersecting b_1b_2 from the region of metastability of the phase γ the latter becomes unstable with respect to the long-range-order parameter. However, the conditions for normal phase transformation into the stable crystalline state have not yet been achieved. In this case the γ-phase, 'overheated' above T_m, should melt, and provided that b_1b_2 is below the glass transition temperature (T_g) the phase γ should transform to an amorphous state.

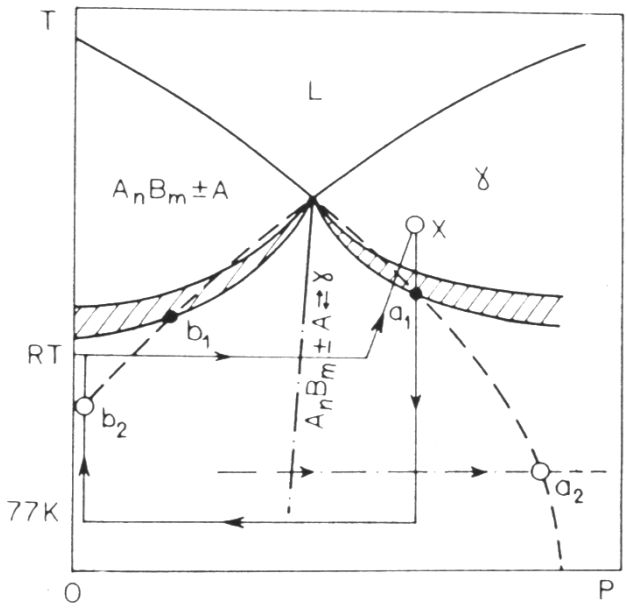

Figure 1. The temperature–pressure phase diagram of a binary A–B system with the stoichiometric semiconductor compound A_nB_m taken from reference [7]. It is explained in the text.

In figure 2, the DSC curves, the volume fraction of the amorphous phase and the relative expansion of the γ-phase sample are shown.

Our goal in this paper is to obtain a description of the relaxation of metastable crystalline phases with competitive formation of a crystalline (stable) and an amorphous (metastable) phase. The model of the phase transformation kinetics (see references [2, 3]) includes expressions derived for the nucleation rates and growth velocities of the phases occurring and for the calculation of the volume fractions of the competing phases. The amorphization

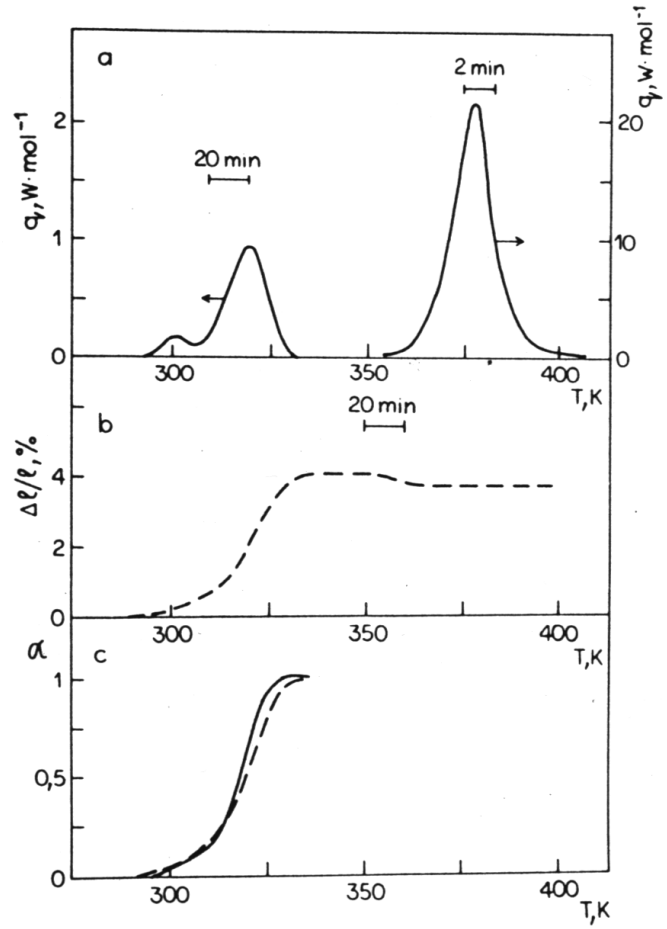

Figure 2. Experimental results from reference [7] for amorphization and crystallization of the HP phase of $Cd_{43}Sb_{57}$ upon heating. (a) Heat release power as a function of temperature; (b) relative expansion of the HP phase sample; (c) volume fraction of the amorphous phase versus temperature. Solid lines denote calorimetric data; dashed lines are the volumetric curves.

from the crystalline phase differs essentially from the solidification of supercooled liquid. The difference lies in the mechanism of nucleation of the new phases. In supercooled liquid, homogeneous nucleation takes place, while in the latter case, nucleation occurs on the boundaries of grains [5, 6]. Phase transformations accompanied by considerable volumetric effects (12% for $Cd_{43}Sb_{57}$ alloy) always start from surface or boundary layers. Accordingly, the derivation of expressions for the nucleation rates and volume fractions of the competing phases has to take this peculiarity into account.

The paper is organized as follows. Section 2 describes the derivation of the volume fraction of the phase nucleating on the boundaries of the grains at time-dependent nucleation rates and growth velocities. In section 3, the problem of the evolution of the volume fractions of two competing phases is considered. In sections 4 and 5, the relations between the thermodynamic functions of phases are considered and the expressions for the nucleation rates and growth velocities as well as equations for the DSC curves are obtained. The application of this approach to experimental results is discussed in section 6.

2. Kinetics of amorphization in a single-phase transformation

Let us first consider the amorphization kinetics in the case of single-phase formation. Then, these results will be extended to the case of competitive nucleation and growth of two phases.

The volume fraction $X(t)$ of a phase nucleating on the grain boundaries was calculated by Cahn [8] in the Johnson–Mehl–Avrami approach [9, 10]. Assuming a spherical shape for the nuclei, constant nucleation rate I and growth velocity u, the volume fraction $X(t)$ is

$$X(t) = 1 - \exp(-X_e(t))$$

where $X_e(t)$ is the 'extended volume' fraction. This is the total volume of growing nuclei without taking into account their overlap. It is given by [8]

$$X_e(t) = 2But \int_0^1 \left\{1 - \exp\left[-\frac{\pi}{3} I_B u^2 t^3 (1 - 3x^2 + 2x^3)\right]\right\} \mathrm{d}x \tag{1}$$

where I_B is the nucleation rate on the boundary per unit of area; B is the area of grain boundaries per unit volume. It is connected with the mean size of the grains by

$$B = \frac{p}{L} \tag{2}$$

where $p = \mathrm{O}(1)$ is a geometrical factor which can be derived for any granular structure. In reference [8] a structural model was used for the determination of B from the mean size of grains L. Assuming that all grains are represented by equal tetracandecahedra (polyhedra whose faces are rectangles and hexagons) and L is the distance between square faces, a value $p = 3.35$ was obtained.

At the early stage of the phase transformation, i.e. $a_B \equiv (I_B u^2)^{1/3} t \ll 1$, the volume fraction of the new phase (1) becomes

$$X(t) = 1 - \exp\left(-\frac{\pi}{3} I_V u^3 t^4\right) \tag{3}$$

where $I_V = B I_B$ is the mean volume nucleation rate. At this stage the phase transformation is similar to a homogeneous bulk nucleation. At the late stage of the transformation, i.e. for $a_B \gg 1$, the asymptotic form of (1) is

$$X(t) = 1 - \exp(-2But) \tag{4}$$

which corresponds to a one-dimensional growth law. The reason for the change in the dependence $X(t)$ at large a_B is the exhaustion of the supply of places at which nucleation can occur on the boundaries, or 'saturation of boundaries' [8], when the boundaries are absorbed by the new phase.

The expression (1) is the basis for the calculation of the kinetics of an isothermal transformation. However, it cannot be used for describing the kinetics of the process of phase transformation in the case when I and u, with their exponential dependences on temperature, cannot be considered to be constant. The time dependence of the growth rate, as will be seen below, results in some peculiarities of the DSC curve which are not present in the case of a constant value of this quantity. Therefore, it is necessary to derive an expression similar to (1) for the case of time-dependent nucleation rates and growth velocities. This derivation will be performed in the mean-field approach of reference [8].

Let us consider a plane parallel to the given boundary at distance y from it. It intersects a spherical grain nucleated on the boundary at the moment t' and has grown to have a radius of

$$R(t, t') = \int_{t'}^{t} u(\tau)\, \mathrm{d}\tau$$

at time t. The intersection area at time t is a circle of radius $[R^2(t,t') - y^2]^{1/2}$ if $R(t,t') > y$, but is zero for evolution times for which $R(t,t') \leqslant y$.

The total area Y_e of all of these intersections determines the extended area [10]. The centres nucleated in the time interval $[t', t' + \mathrm{d}t']$ on unit area of the boundary give the following contribution to Y_e:

$$\mathrm{d}Y_e(t) = \begin{cases} \pi I_B(t') \left[R^2(t,t') - y^2\right] \mathrm{d}t' & R(t',t) > y \\ 0 & R(t',t) < y. \end{cases} \tag{5}$$

Integrating, we obtain

$$Y_e(y,t) = \pi \int_0^{t_m(t,y)} I_B(t') \left[R^2(t,t') - y^2\right] \mathrm{d}t' \tag{6}$$

where $t_m(t,y)$ is determined by the relation

$$R(t_m, t) = y. \tag{7}$$

As the nuclei are distributed randomly on the plane, the connection of the actual area with the extended one is given by the following relation (see equation (1)) for the volume fraction:

$$Y(y,t) = 1 - \exp(-Y_e(y,t)). \tag{8}$$

The total transformed volume fraction per unit of area of the given boundary is found by integrating (8) with respect to y:

$$\begin{aligned} Y_{tot}(t) &= 2\int_0^{\infty} Y(y,t)\,\mathrm{d}y \\ &= 2\int_0^{y_m(t)} \left\{1 - \exp\left[-\pi \int_0^{t_m(t,y)} I(t')(R^2(t',t) - y^2)\,\mathrm{d}t'\right]\right\} \mathrm{d}y. \end{aligned} \tag{9}$$

We introduce the dimensionless variable $x = y/y_m(t)$ and rewrite expressions (9) and (7) as

$$Y_{tot}(t) = 2y_m(t) \int_0^1 \left\{1 - \exp\left[-\pi \int_0^{t_m(t,x)} I_B(t') \left[R^2(t',t) - y_m^2(t)x^2\right] \mathrm{d}t'\right]\right\} \mathrm{d}x \tag{10}$$

$$R(t_m, t) = xR(0,t).$$

If the boundaries are distributed chaotically in the volume, the quantity $X_e = BY_{tot}$ is the extended volume for our problem, so the real volume X of transformed material is $1 - \exp(-X_e)$; that is,

$$X(t) = 1 - \exp[-BY_{tot}(t)]. \tag{11}$$

If the argument of the exponential function in (9) is small, we have

$$BY_{tot}(t) = 2\pi B \int_0^{y_m(t)} \mathrm{d}y \int_0^{t_m(t,y)} I_B(t') \left[R^2(t',t) - y^2(t)\right] \mathrm{d}t'. \tag{12}$$

Changing the order of integration in equation (12), it is not difficult to obtain

$$Y_{tot}(t) = \frac{4\pi}{3} \int_0^t I_B(t') R^3(t',t)\,\mathrm{d}t' \tag{13}$$

so expression (11) becomes

$$X(t) = 1 - \exp\left[-\int_0^t I_V(t') V(t',t)\,\mathrm{d}t'\right] \tag{14}$$

where $V(t',t) = (4\pi/3)R^3(t',t)$.

In the limiting case of a large argument of the exponential function in (9), we have

$$X(t) = 1 - \exp\left[-2By_m(t)\right]. \tag{15}$$

Expressions (14) and (15) generalize (3) and (4) respectively.

The equilibrium shape of a nucleus is not necessary spherical. In the general case, for example, if there are elastic stresses in the initial phase, it is described by several parameters. The values of these parameters for the critical nucleus are determined from the condition of having a minimum of the free energy if the shape is varied. Also, the growth velocity of a nucleus can be anisotropic. Therefore, we also consider the model with cylindrical form for the nuclei. Let the growth velocities of a grain along the boundary and perpendicular to it be equal respectively to $u_\tau(t)$ and $u_n(t)$. Then the radius of the grain and its height are

$$r(t', t) = \int_{t'}^{t} u_\tau(t'')\,\mathrm{d}t'' \qquad z(t', t) = \int_{t'}^{t} u_n(t'')\,\mathrm{d}t''.$$

Calculations similar to those performed above give the following expression for $Y_{tot}(t)$:

$$Y_{tot}(t) = 2\int_0^{y_m(t)} \left\{1 - \exp\left[-\pi \int_0^{t_m(t,y)} I_B(t')r^2(t', t)\,\mathrm{d}t'\right]\right\} \mathrm{d}y. \tag{16}$$

Here, $y_m \equiv z(0, t)$ and $t_m(t, y)$ is determined by the equation $z(t_m, t) = y$.

3. Evolution of the volume fractions of competing phases nucleating on the boundaries of grains

Expression (1) can be generalized to the case of simultaneous growth of two phases. For simplicity, we consider the case of constant nucleation rates I_k and growth velocities u_k, with $u_2 > u_1$.

The expressions for the extended areas of k-phases, similar to (5) and (6), have the following forms:

$$\mathrm{d}Y_k^e = \begin{cases} \pi I_k^B \left[u_k^2(t' - t)^2 - y^2\right] \mathrm{d}t' & u_k(t - t') > y \\ 0 & u_k(t - t') < y \end{cases} \tag{17}$$

$$Y_k^e = \int_0^t \mathrm{d}Y_k^e = \pi I_k^B \int_0^{t - y/u_k} \left[u_k^2(t - t')^2 - y^2\right] \mathrm{d}t'. \tag{18}$$

By integration of (18) and with the substitution $\xi_k = y/u_k t$, we obtain

$$Y_k^e = \pi I_k^B u_k^2 t^3 \left[\frac{1 - \xi_k^3}{3} - \xi_k^2(1 - \xi_k)\right]. \tag{19}$$

The connection between the actual area Y_k and the extended one in the mean-field approximation [8–10] is given by the following set of equations [2]:

$$\begin{aligned} &\mathrm{d}Y_k(t) = [1 - Y(t)]\ \mathrm{d}Y_k^e(t) \qquad k = 1, 2 \\ &Y = Y_1 + Y_2 \end{aligned} \tag{20}$$

whence we find

$$Y = 1 - \exp[-(Y_1^e + Y_2^e)]. \tag{21}$$

By integrating (20) with respect to y, we find the increase of the volume $\mathrm{d}V_k$ of the k-phase during the time $\mathrm{d}t$. Taking into account that $\dot{Y}_k^e \equiv \mathrm{d}Y_k^e/\mathrm{d}t = \pi I_k^B u_k^2 t^2(1 - \xi_k^2)$, one has

$$\mathrm{d}V_k = 2\left[\int_0^\infty \dot{Y}_k^e \exp(-Y_1^e - Y_2^e)\,\mathrm{d}y\right] \mathrm{d}t$$

or

$$\mathrm{d}V_1(t) = 2\pi I_1^B u_1^2 t^3\,\mathrm{d}t \int_0^1 (1-x^2)\exp\left(-\frac{\pi}{3}t^3(\alpha-\beta x^2+\gamma x^3)\right)\mathrm{d}x$$

$$\mathrm{d}V_2(t) = 2\pi I_2^B u_2^2 t^3\,\mathrm{d}t \left\{u_1\int_0^1\left[1-\left(\frac{u_1}{u_2}\right)^2 x^2\right]\exp\left(-\frac{\pi}{3}t^3(\alpha-\beta x^2+\gamma x^3)\right)\mathrm{d}x \right. \tag{22}$$
$$\left. + u_2\int_{u_1/u_2}^1 (1-x^2)\exp\left(-\frac{\pi}{3}I_2^B u_2^2 t^3(1-3x^2+2x^3)\right)\mathrm{d}x\right\}$$

where

$$\alpha \equiv I_1u_1^2 + I_2u_2^2$$
$$\beta \equiv 3(I_1+I_2)u_1^2$$
$$\gamma \equiv 2(I_1u_1^2 + I_2u_1^3/u_2).$$

It was taken into account in the integration with respect to y that the layer of the k-phase is in the interval $[0, y_k]$, where $y_k = u_k t$. For $V = V_1 + V_2$, we have

$$V = 2\int_0^\infty Y\,\mathrm{d}y = 2\int_0^{y_1}\left[1-\exp(-(Y_1^e+Y_2^e))\right] + 2\int_{y_1}^{y_2}\left[1-\exp(-Y_2^e)\right]\mathrm{d}y$$

or

$$V(t) = 2u_2 t\left\{\frac{u_1}{u_2}\int_0^1\left[1-\exp\left(-\frac{\pi}{3}t^3(\alpha-\beta x^2+\gamma x^3)\right)\right]\mathrm{d}x \right.$$
$$\left. + \int_{u_1/u_2}^1\left[1-\exp\left(-\frac{\pi}{3}I_2u_2^2t^3(1-3x^2+2x^3)\right)\right]\mathrm{d}x\right\}. \tag{23}$$

The expressions for $V_k(t)$ are obtained by integrating (22) with respect to t.

The extended volume X_k^e of the k-phase per unit volume of a system is BV_k. Assuming that the boundaries are distributed chaotically in space, we have the following equations for the volume fractions being sought in the mean-field approximation [2]:

$$\mathrm{d}X_k = (1-X)\,\mathrm{d}X_k^e \qquad X = X_1 + X_2.$$

From these we obtain

$$X(t) = 1 - \exp(-BV(t)) \tag{24}$$

$$X_k(t) = B\int_0^1 \dot{V}_k(t')\exp(-BV(t'))\,\mathrm{d}t' \tag{25}$$

where $\dot{V}_k(t) \equiv \mathrm{d}V_k(t)/\mathrm{d}t$ and $V(t)$ are given by expressions (22) and (23) respectively.

Let us introduce the characteristic time t^* of exhaustion of nucleation sites by means of the conditions

$$a_B^{(1)^3} + a_B^{(2)^3} \approx 1 \qquad a_B^{(k)} = (I_k u_k^2)^{1/3}t \qquad t^* = (I_1u_1^2 + I_2u_2^2)^{-1/3}$$

and consider limiting cases of expression (24). At $t < t^*$ (the arguments of the exponential functions in (23) are small), we have

$$X(t) = \frac{\pi}{3}(I_1^{(V)}u_1^3 + I_2^{(V)}u_2^3)t^4.$$

For $t \gg t^*$,

$$X(t) = 1 - \exp(-2Bu_2t). \tag{26}$$

Thus, at large times, the kinetics of transformation is determined by the growth of the fast-growing phase. This means that the layer of the first phase appears 'immured' inside the

layer of the second phase and does not make a contribution to the increment of the transformed volume. This result is obtained on the assumption that the quantities $a_B^{(1)}$ and $a_B^{(2)}$ are of the same order. If $a_B^{(1)^3} \gg 1$ and $a_B^{(2)^3} \ll 1$, then we have the following expression instead of (26):

$$X(t) = 1 - \exp(-2Bu_1 t). \tag{27}$$

In this case, the growth of the transformed region is determined by the slow-growing phase if its nucleation rate significantly exceeds the nucleation rate of the fast-growing phase: $I_1 u_1^2 \gg I_2 u_2^2$. The reason for this is the exhaustion of the supply of places at which nucleation of the first phase can occur.

4. Nucleation rates and growth velocities of the phases formed

Nucleation on the boundaries of grains is a particular case of heterogeneous nucleation, and the expression for the free energy of k-phase critical nucleus formation is [11]

$$\Delta G_{*,k}^B = \Delta G_{*,k}^H f(\kappa_k) \tag{28}$$

where $\Delta G_{*,k}^H$ is the free energy of k-phase critical nucleus formation for homogeneous nucleation; $f(\kappa) \equiv \frac{1}{2}(2 - 3\kappa + \kappa^3)$; $\kappa_k \equiv \cos\theta = \sigma_{ii}/2\sigma_{ik}$; θ is the contact angle; σ_{ii} is the energy of the grain boundaries in the initial (i) phase which is the HP phase; σ_{ik} is the surface tension of the interface between phases i and k.

The expression for the rate of homogeneous nucleation of the k-phase has the following form [2, 3]:

$$I_k^H(T) = 2N\nu_0 \left(\frac{\sigma_i a^2}{kT}\right)^{1/2} \exp[-(\Delta g(T) + \Delta G_{*,k}^H(T))/kT] \tag{29}$$

where $\Delta g(T)$ is the activation free energy of self-diffusion in the initial phase; ν_0 is the frequency of atom oscillations; N is the normalization factor which is approximately equal to the number of atoms in unit volume; a is the mean interatomic distance.

The expression for the nucleation rate on the boundary, following [11], is obtained from (29) by replacing $\Delta G_{*,k}^H$ by $\Delta G_{*,k}^B$ and the factor N by N^B (N^B is the number of atoms on the given surface in unit volume):

$$I_k^B(T) = 2N^B\nu_0 \left(\frac{(1-\kappa)^2}{f(\kappa)}\frac{\sigma_{ik}a^2}{kT}\right)^{1/2} \exp[-(\Delta g(T) + \Delta G_{*,k}^B(T))/kT]. \tag{30}$$

This expression differs from that of reference [11] by the addition of the pre-exponential factor

$$z_k n_{s,k}^* = \{[(1-\kappa)^2/f(\kappa)][\sigma_{ik}a^2/kT]\}^{1/2}$$

where z_k is Zel'dovich factor, $n_{s,k}^*$ is the number of atoms on the critical nucleus surface. This factor was calculated using the formula for the free energy and geometric coefficients which are given in [11].

The free energy of critical nucleus formation is

$$\Delta G_{*,k}^H = \frac{16\pi}{3}\frac{\sigma_{ik}^3}{\Delta\mu_{ik}^2} \tag{31}$$

where $\Delta\mu_{ik} = \mu_i(T) - \mu_k(T)$ is the difference of chemical potentials of atoms in the phases i and k.

The growth velocity of a k-phase nucleus is also expressed through the function $\Delta\mu_{ik}(T)$ [11]:

$$u_k(T) = a\nu_0 \exp\left(-\frac{\Delta g(T)}{kT}\right)\left[1 - \exp\left(-\frac{\Delta\mu_{ik}(T)}{kT}\right)\right]. \tag{32}$$

The expected temperature dependences of the chemical potentials of atoms in different phases at fixed pressure for the alloy considered are represented schematically in figure 3. For differences of chemical potentials $\Delta\mu_{ik}$, it is possible to use an expression in the form of an expansion in a series in the vicinity of an appropriate temperature T_0:

$$\Delta\mu_{ik}(T) = \Delta\mu_{ik}(T_0) + \frac{\partial\,\Delta\mu_{ik}}{\partial T}\bigg|_{T=T_0}(T-T_0) + \frac{1}{2}\frac{\partial^2\,\Delta\mu_{ik}}{\partial T^2}\bigg|_{T=T_0}(T-T_0)^2$$
$$\equiv \Delta\mu_{ik}^{(0)} - \Delta s_{ik}^{(0)}(T-T_0) - \frac{\Delta c_{p,ik}^{(0)}}{2T_0}(T-T_0)^2 \tag{33}$$

where $\Delta\mu_{ik}^{(0)}$, $\Delta s_{ik}^{(0)}$ and $\Delta c_{p,ik}^{(0)}$ are differences of chemical potentials, entropies and heat capacities of phases i and k at the temperature T_0. From this, using the thermodynamic relations $\Delta\mu = \Delta h - T\,\Delta s$ and $\Delta s = -\partial\,\Delta\mu/\partial T$, we derive expressions for the differences of entropies and enthalpies of phases i and k:

$$\begin{aligned}
\Delta s_{ik}(T) &= \Delta s_{ik}^{(0)} + \frac{\Delta c_{p,ik}^{(0)}}{T_0}(T-T_0)\\
\Delta h_{ik}(T) &= \Delta h_{ik}^{(0)} + \frac{\Delta c_{p,ik}^{(0)}}{2T_0}(T^2-T_0^2)\\
\Delta h_{ik}^{(0)} &= \Delta\mu_{ik}^{(0)} + \Delta s_{ik}^{(0)}\,T_0.
\end{aligned} \tag{34}$$

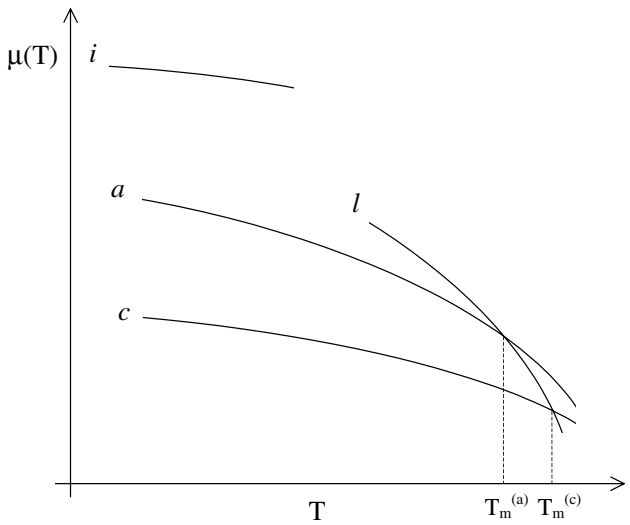

Figure 3. Schematic temperature dependences of the chemical potentials of an atom in different phases at a fixed pressure (1 bar). Lines i, a, c and l correspond to the initial (HP), amorphous, stable crystalline and liquid phases. $T_m^{(c)}$ is the melting temperature of the stable crystalline phase, $T_m^{(a)}$ the analogous temperature for the amorphous phase.

A similar expansion can also be obtained for the surface tension of the interface of phases i and k:

$$\sigma_{ik}(T) = \sigma_{ik}^{(0)} - \chi(T-T_0) \tag{35}$$

where $\sigma_{ik}^{(0)} \equiv \sigma_{ik}(T_0)$ and $\chi \equiv -(\partial\sigma_{ik}/\partial T)\big|_{T=T_0}$.

In that case, when the phase transformation occurs near an equilibrium point of the phases, as, for example, in the case of supercooled liquid, it is natural to carry out the expansion of $\Delta\mu_{ik}(T)$ in the vicinity of this point. In this case $\Delta\mu_{ik}^{(0)} = 0$ and $\Delta s_{ik}^{(0)} = \Delta h_{ik}^{(0)}/T_0$ ($\Delta h_{ik}^{(0)}$ is the heat of phase transition). In our case (see figure 3) it is not clear whether the curves of the HP and amorphous phases intersect somewhere in the low-temperature region. Also, the virtual equilibrium point T_{eq} of the amorphous and stable crystalline phases is far ($T_{eq} > T_m^{(c)}$) from the temperature of the onset of the amorphous phase crystallization process ($\approx 0.5 T_m^{(c)}$). Therefore, we use the expansion of $\Delta\mu_{ik}(T)$ in the form of (33), where T_0 is the temperature of the onset of the corresponding phase transformation. It is sufficient to take the linear approximation, as the temperature intervals of the transformations are comparatively small.

The relation between the surface tensions of the amorphous and crystalline phases (σ_{ia} and σ_{ic} respectively) plays an important role in competitive nucleation. It was obtained in references [1, 3] and has the form

$$\sigma_{ia} = \sigma_{ic} - T\xi \tag{36}$$

where ξ is the configurational entropy per atom on the surface of the amorphous phase nucleus (cluster). This relation can be explained by the following reasoning.

In translationally invariant crystalline structures, configurational entropy is produced by defects and is small due to the large formation energies of the point and extended defects. In amorphous solids the residual entropy at $T \to 0$ is due to the contribution of the configurational entropy. Usually it is not small; $\xi \sim 1$. The growing cluster can build its surface layer in many ways, $\sim \exp(\xi N_s)$, where N_s is the number of atoms in the surface layer. Thus the configurational entropy lowers the surface free energy of a cluster and correspondingly increases the nucleation rate.

5. The equation of the DSC curve

In order to derive the DSC curve equation, we assume a linear dependence of the quantity of heat released during $\mathrm{d}t$ on the increment of the transformed volume:

$$\mathrm{d}Q = \Delta h(T)\,\mathrm{d}X \tag{37}$$

where $\Delta h(T)$ is the heat of transformation (expression (34) for $\Delta h_{ik}(T)$ is an approximation for this function). Then the equation of the DSC curve for nucleation on the boundaries of grains is obtained using (11) and (10) (or (16)):

$$q(t) \equiv \frac{\mathrm{d}Q}{\mathrm{d}t} = \Delta h(T)\, B \frac{\mathrm{d}Y_{tot}(t)}{\mathrm{d}t} \exp(-BY_{tot}(t)) \tag{38}$$

$$\frac{\mathrm{d}Y_{tot}(t)}{\mathrm{d}t} = 2u(t)\left[\int_0^1 \mathrm{d}x\ \{1 - \exp(-f(x,t))\} + 2y_m(t)\int_0^1 \mathrm{d}x\ \frac{\partial f(x,t)}{\partial t}\{\exp(-f(x,t))\}\right] \tag{39}$$

where

$$f(x,t) = \pi \int_0^{t_m(t,x)} I(t')\left[R^2(t',t) - y_m^2(t)x^2\right]\mathrm{d}t'.$$

On heating at a constant rate λ starting from temperature T_i, i.e. with

$$T = T_i + \lambda t \tag{40}$$

these relations give a dependence of q on T.

In the case of constant values of the quantities I and u, expression (39) has the following form:

$$\frac{\mathrm{d}Y_{tot}(t)}{\mathrm{d}t} = 2u\int_0^1 \left\{1 - \exp\left(-\frac{\pi}{3} I_B u^2 t^3 \left[1 - 3x^2 + 2x^3\right]\right) \mathrm{d}x\right\} + 2\pi I u^3 t^3 \int_0^1 \left[1 - 3x^2 + 2x^3\right] \exp\left(-\frac{\pi}{3} I_B u^2 t^3 \left[1 - 3x^2 + 2x^3\right]\right) \mathrm{d}x. \quad (41)$$

This function increases $\sim t^3$ at small times, then it passes through the maximum corresponding to the stage of saturation of the boundaries and tends to a constant value equal to $2u$ at large times. The main distinction of the function (39) from (41) appears at large times: it continues to increase as $2u(t)$. The DSC curve becomes one which has either an additional peak or a fracture in the ascending branch. Thus, the dependence of the grain growth velocity on time results in a change of the usual form of the DSC peak.

The DSC curve equation involves a number of phenomenological parameters whose exact values are not known. Therefore it is desirable to simplify the model, in order to exclude some of the parameters. Such a simplification is possible for Cd–Sb alloy due to the following features of the amorphization DSC curve (figure 2). Noting that the two peaks of this curve are considerably separated, we can conclude that the saturation of boundaries occurs in a narrow temperature range (about 10 K) and finishes at a volume fraction of about 0.1. Consequently, the nucleation and growth rates in this short stage may be taken as constant, equal to some mean values $\bar{I}$, $\bar{u}_\tau$ and $\bar{u}_n$. The second peak is apparently related to the stage of one-dimensional growth of the boundary layer and can be described by just the function $u_n(t)$. As a result, expression (16) can be approximately replaced by the following one:

$$Y_{tot}(t) = 2y_m(t)\int_0^1 \left[1 - \mathrm{e}^{-\alpha t^3(1-x^3)}\right] \mathrm{d}x \quad (42)$$

where $a = (\pi/3)\bar{I}\bar{u}_\tau^2$.

Correspondingly, the DSC curve equation takes the following form:

$$q_{am}(t) = 2B\,\Delta h(T)\,\mathrm{e}^{-BY_{tot}(t)}\left\{3\alpha t^2 y_m(t)\int_0^1 \mathrm{d}x\ \mathrm{e}^{-\alpha t^3(1-x^3)} + u_n(t)\int_0^1 \mathrm{d}x\ \left[1 - \mathrm{e}^{-\alpha t^3(1-x^3)}\right]\right\}. \quad (43)$$

The first and second terms describe respectively the first and second peaks. The first peak can be distinct if the growth velocity $u_n(t)$ increases sufficiently slowly at the first stage of the process.

The equation of the DSC curve for random nucleation in the volume is obtained using equation (14):

$$q_{cr}(t) = 4\pi\,\Delta h(T)\,u(t)\left[\int_0^t I_V(t')R^2(t',t)\,\mathrm{d}t'\right]\exp\left(-\int_0^t I_V(t')V(t',t)\,\mathrm{d}t'\right). \quad (44)$$

6. Discussion

The expressions obtained in the previous sections give a complete description of the kinetics of metastable crystalline phase polymorphic transformation with competitive formation of amorphous (metastable) and crystalline (stable) phases. Along with the description of the evolution of the volume fractions of the phases formed, the expressions for the DSC curves have also been obtained, which allows one to carry out a quantitative analysis of the calorimetric measurements.

In references [5, 6], the authors, on the basis of the analysis of experimental data from measurements of the electrical resistance of the sample at various stages of amorphization, conclude that nucleation of the amorphous phase occurs on the boundaries of grains of the initial phase. The measured value of the Avrami index, 1.4 ± 0.4 [5], shows that one-dimensional growth takes place. As shown above, the form of the experimental amorphization DSC curve agrees with this conclusion. The rather large volumetric effect of $Cd_{43}Sb_{57}$ amorphization hinders the formation of nuclei in the bulk because of the appearance of elastic stresses. Along with this, the boundaries provide relaxation of the stresses due to diffusion and the emission and absorption of dislocation loops. The diminishing of stresses due to the relaxation process together with the decrease in surface energy considered above by means of the function $f(\kappa)$ lead to the nucleation rate on boundaries being much larger than that in grain bulk.

The volume changes due to amorphization lead to plastic deformation of the material. As is seen (figure 2), the amorphization proceeds at comparatively low temperatures (300–330 K). The bulk diffusion activation energy for this type of alloy is 1.5–2 eV [5]. It considerably exceeds Δg, which controls the growth rate. Taking this into account, as well as the geometry of the growing phase, we conclude that the main role as regards the stress relaxation is taken by the boundary and interfacial diffusion. This is Coble diffusional–viscous flow of the material.

In addition to the nuclei of the amorphous phase, nuclei of the stable crystalline phase are also formed on the boundaries of grains, and, as follows from figure 3 and expression (32), the growth rate of the latter is greater than that of the former. However, x-ray analysis of the sample at the first stage of transformation [5] shows that its structure is amorphous, and there are no inclusions of the crystalline phase. The transition into the basic crystalline state occurs from this amorphous phase at higher temperatures by random nucleation in a bulk. Using the results of section 4, we conclude that the rate of nucleation of crystallites is negligible in comparison with that of clusters for competitive nucleation. The reason for this is that the surface tension of clusters is less than that of crystallites (see relation (36)). Moreover, the dominance of the nucleation rate of clusters in this case is expressed more by the strength than in the case of the homogeneous nucleation mechanism, since the height of the barrier $\Delta G^B_{*,a}$ for nucleation of clusters is lowered further by the $f(\kappa)$ function, which decreases with decreasing surface tension.

Despite the values of the parameters controlling nucleation and growth of the phases forming being unknown, they can easily be chosen to fit the experimental data. Reasonable values of the parameters for amorphization are as follows: temperature of melting of the stable crystalline phase of the $Cd_{43}Sb_{57}$ alloy $T_m^{(c)} = 723$ K; $a = 2.83 \times 10^{-8}$ cm; mean grain size $L = 3 \times 10^{-5}$ cm; $\alpha = 10^{-8}$ s^{-3}. The linear approximation with factors $\Delta\mu_{ia}^{(0)}/kT_m^{(c)} = 0.6$, $\Delta s_{ia}^{(0)}/k = -0.9$, $T_0 = 275$ K was used for the difference of chemical potentials. The function $u_n(t)$ was taken in the form (32) with

$$\Delta g(T) = \Delta g_0(1 - \epsilon(T - T_0)/T_m^{(c)}).$$

The best fit is provided by the values $\Delta g_0/kT_m^{(c)} = 14.8$ (about 0.9 eV) and $\epsilon = 2.5$. The second term in this expression describes a weak temperature dependence of the activation free energy.

We used the following for the crystallization: $\Delta g/kT_m^{(c)} = 10.2$; $\sigma_{ac}a^2/kT_m^{(c)} = 0.65$; $\Delta\mu_{ac}^{(0)}/kT_m^{(c)} = 0.4$; $\Delta s_{ac}^{(0)}/k = 0.8$; $T_0 = 340$ K. Note that simultaneous changes of the values of several quantities can affect the result weakly.

The computational DSC curves and temperature dependences of the volume fractions for the processes of amorphization and crystallization presented in figure 4 are in agreement with those obtained experimentally. Equation (43) of the model with plate-like [11] shape of the nuclei was used for the amorphization DSC curve. Thus the transformation seems to

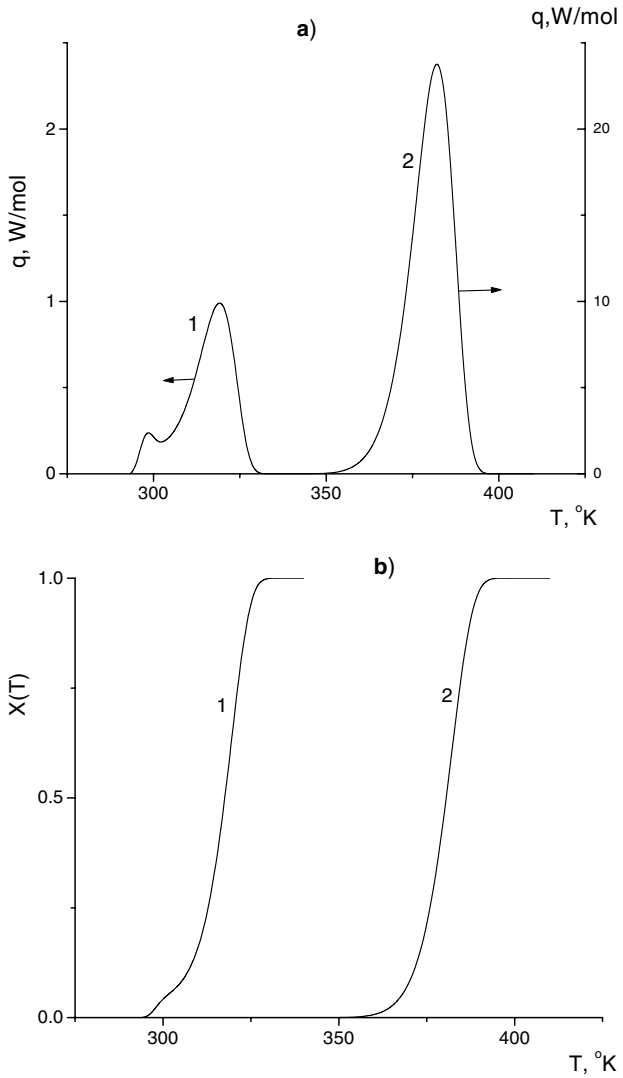

Figure 4. (a) Calculated DSC curves for the following processes for the $Cd_{43}Sb_{57}$ alloy: HP phase amorphization (1) and amorphous phase crystallization (2). (b) Volume fractions of the amorphous (1) and crystalline (2) phases versus temperature.

proceed as follows. The amorphous phase precipitates grow mainly along the boundaries, gradually covering grains with a thin layer. Then an increase in thickness of this layer occurs. Equation (43) for appropriately chosen quantities describes such a process adequately.

Acknowledgments

We thank E G Ponyatovsky for useful discussions and A A Turkin for valuable technical assistance. This work was carried out with financial support from the Ukrainian Centre of Science and Technology, Project N442.

References

[1] Bakai A S 1994 *Fiz. Nizk. Temp.* **20** 469 (Engl. Transl. 1994 *Ukr. J. Low Temp. Phys.* **20** 373)
Bakai A S 1994 *Fiz. Nizk. Temp.* **20** 477 (Engl. Transl. 1994 *Ukr. J. Low Temp. Phys.* **20** 379)

[2] Alekseechkin N V, Bakai A S and Lazarev N P 1995 *Fiz. Nizk. Temp.* **21** 565 (Engl. Transl. 1995 *Ukr. J. Low Temp. Phys.* **21** 440)

[3] Alekseechkin N V, Bakai A S and Abromeit C 1998 *Metallofiz. Nov. Technol.* **20** 15 (Engl. Transl. 1999 *Ukr. J. Met. Phys. Adv. Technol.* **18** 619)

[4] Blatter A and Allmen M 1986 *Proc. 6th Int. Conf. on Liquid and Amorphous Metals (Garmisch-Partenkirchen, Germany)* vol 2, p 245

[5] Ponyatovsky E G, Belash I T and Barkalov O I 1989 *Proc. 7th Int. Conf. on Liquid and Amorphous Metals (Kyoto, Japan)* p 679

[6] Barkalov O I, Belash I T, Gantmacher V F, Ponyatovsky E G and Teplinsky V M 1988 *Pis. Zh. Eksp. Teor. Fiz.* **48** 561

[7] Ponyatovsky E G and Barkalov O I 1992 *Mater. Sci. Rep.* **8** 147

[8] Cahn J W 1956 *Acta Metall.* **4** 449

[9] Johnson W A and Mehl R F 1939 *Trans. AIME* **135** 416

[10] Avrami M 1939 *J. Chem. Phys.* **7** 1103
Avrami M 1939 *J. Chem. Phys.* **8** 212
Avrami M 1941 *J. Chem. Phys.* **9** 177

[11] Christian J W 1965 *The Theory of Transformations in Metals and Alloys* (Oxford: Pergamon)